A Comparison of Micromachined Inductors with Different Magnetic Core Materials

Jae Y. Park* and Mark G. Allen
School of Electrical and Computer Engineering
Georgia Institute of Technology
Atlanta, GA 30332-0250
*Office: (404) 894-9907, Fax: (404) 894-5028, E-mail: gt1216a@prism.gatech.edu

ABSTRACT

Two integrated inductors with different electroplated cores, permalloy (Ni(80%)-Fe(20%)) and orthonol (Ni(50%)-Fe(50%)) cores, are designed, fabricated, tested, and compared in order to reach optimum designs for integrated inductors and transformers. These integrated inductors were realized on a silicon wafer by using micromachining techniques to fabricate wrapped coils wound around a 'bar' of high permeability core material [1-2]. These devices have high current capability (up to 2A steady DC current) and are suitable for application in DC/DC converters. The total inductor size is 4 mm x 1.0 mm x 0.13 mm having 30 turns of multilevel copper coils (40 μm thick). Each inductor has nominally identical geometry and core thickness (15 μm), implying that differences in performance would be due entirely to differences in core behavior. The permalloy core inductor has a slightly higher inductance than the orthonol core inductor. However, the DC saturation current of the orthonol core inductor is much higher than the permalloy core inductor. In many high power applications, high saturation flux density is more important than permeability, because DC saturation current is proportional to saturation flux density. The measured behavior confirms on *in-situ* electroplated samples and fabricated components the trends expected from bulk properties of these nickel-iron alloys.

INTRODUCTION

Applications such as sensors, filters, and integrated micromagnetic power devices (e.g., miniaturized switched DC/DC power converters integrated with multichip modules or electronic systems) demand new microinductors which have high values of inductance, saturation current, and Q-factor [3-7]. In particular, high frequency, high density, and high efficiency DC/DC power converters using micromachined inductors [8-10] are needed for use in communications, military/aerospace applications, and computer/peripheral or other portable devices. Requirements on power converters of high efficiency, small size, low weight, and lower cost will require that switching frequencies increase. At such high switching frequencies, miniaturized surface-mount magnetic components [10-11] may be able to be replaced by fully integrated magnetic devices. However, magnetic properties of electroplated cores for such devices may be very different from magnetic properties of the bulk magnetic materials, thus necessitating an *in-situ* test. In this paper, two integrated micromachined inductors for this application are fabricated with different magnetic core materials in order to assess the utility of these materials in integrated inductor realization.

Desirable characteristics of magnetic cores for integrated power inductors and transformers can be summarized as follows: first, high saturation flux in order to obtain high saturation current; second, high permeability to obtain high inductance; third, high resistivity to reduce eddy current loss. In addition, micromachined inductors should be designed to have a completely closed magnetic circuit to minimize leakage flux, since leakage flux does not contribute to the total inductance of the device and can cause interference with other integrated circuitry on the same substrate.

DESIGN AND MODELING

Figure 1 shows the proposed inductive component which is composed of a magnetic core and multilevel metal interconnections.

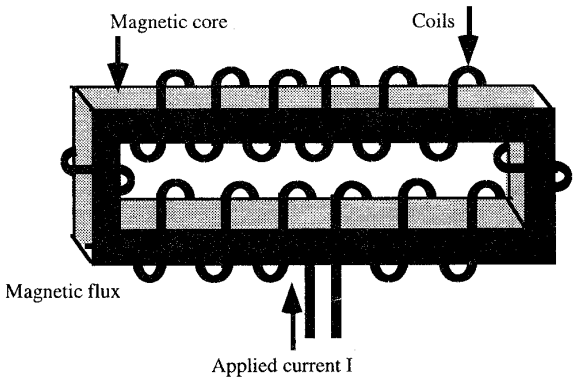

Figure 1. Schematic diagram of a fully integrated micromachined inductor

In order to wrap the magnetic core with the conductor coils on a planar surface, a multilevel metallization scheme is used. Lower conductor lines are deposited using electroplating techniques and insulated. A magnetic core is deposited using electroplating and insulated. Via connections to the lower conductor lines are defined and filled using electroplating. Finally, the upper conductor lines are deposited using electroplating. The procedure for fabrication will be described in more detail later.

The calculation of the inductance for the structure depicted in Figure 1 is straightforward. The inductance L and reluctance R of the integrated inductor are expressed as the following:

$$R = \frac{\ell_c}{\mu_0 \mu_r A_c} \quad (1)$$

$$L = \frac{\mu_0 \mu_r A_c N^2}{\ell_c} = \frac{N^2}{R} \quad (2)$$

where A_c is the cross-sectional area of the film magnetic core, ℓ_c is the length of the closed magnetic core, N is the number of coil turns, and μ_0 and μ_r are the permeability of the vacuum and the relative permeability of the magnetic core, respectively. The quality factor can be defined as:

$$Q = \frac{\omega L}{\text{resistance}} = \frac{\omega \mu_0 \mu_r N A_c A_w}{2\rho W \ell_c} \quad (3)$$

where A_w is the cross-sectional area of the conductor, ω is the radian frequency, W is the width of the film magnetic core, and ρ is the conductivity of the conductor material. From the above equations (2) and (3), it is concluded that inductance and Q-factor are linearly proportional to μ_r in this micromachined inductor.

An additional quantity of importance in power applications is the saturation current of the inductor (i.e., the current at which the inductor saturates magnetically). The saturation current can be determined from the equations:

$$\Phi = BA_c = \frac{NI}{R} \quad (4)$$

$$I_{sat} = \frac{B_{sat} R A_c}{N} \quad (5)$$

As shown in the above equations 4 and 5, it is clear that saturation flux density is proportional to DC saturation current. Thus, the micromachined inductor composed of magnetic core with high saturation flux density is appropriate to high power applications. Eddy current losses in the magnetic core as well as the skin depth effect in the conductor are neglected in these calculations. This assumption is reasonable since integrated inductors fabricated using IC technology are composed of cores and conductor lines whose thickness is on the order of several tens of microns, and are operating typically at low (< 10 MHz) frequencies in DC/DC converter applications.

MAGNETIC CORE MATERIALS

Inductors such as the one shown schematically in Figure 1 have been realized previously using *permalloy* (80% nickel - 20% iron) cores. It is known that other alloy compositions of the nickel-iron system have higher saturation flux densities. For example, the 50% nickel - 50% iron alloy, known as *orthonol*, has a saturation flux density on the order of 50% higher than permalloy in the bulk [12]. In order to assess the suitability of orthonol as a magnetic material for micromachined inductors, samples of both permalloy and orthonol were deposited using electroplating and characterized using a vibrating sample magnetometer.

The fabrication procedure for the preparation of core samples is as follows. A seed layer consisting of 200 Å chromium, 1500 Å copper, and 400 Å chromium was deposited on a silicon wafer using electron beam evaporation. A 15 μm thick photoresist layer (Shipley STR-1110) was deposited on top of the seed layer and patterned to form sample molds 12 mm by 4 mm in area. The magnetic materials were then deposited using electroplating using the parameters in Table I. The core samples were then removed from the wafer using wet chemical etching. Figures 2 and 3 show magnetic B-H (flux density - magnetic field strength) curves as measured by a vibrating sample magnetometer at low frequency for each material.

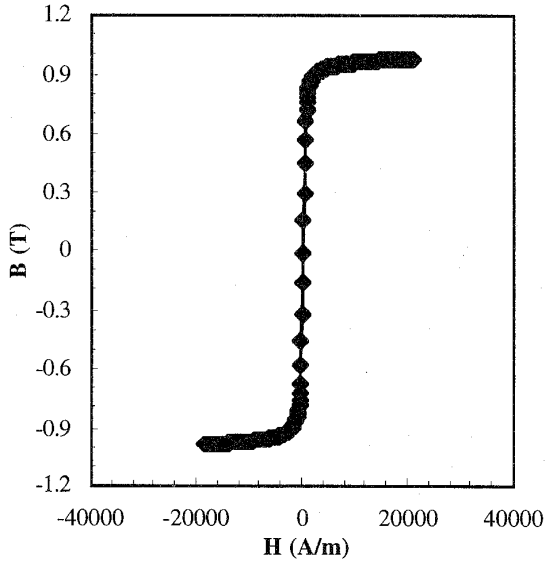

Figure 2. Flux density versus magnetic field intensity curve for fabricated permalloy (80/20) test samples

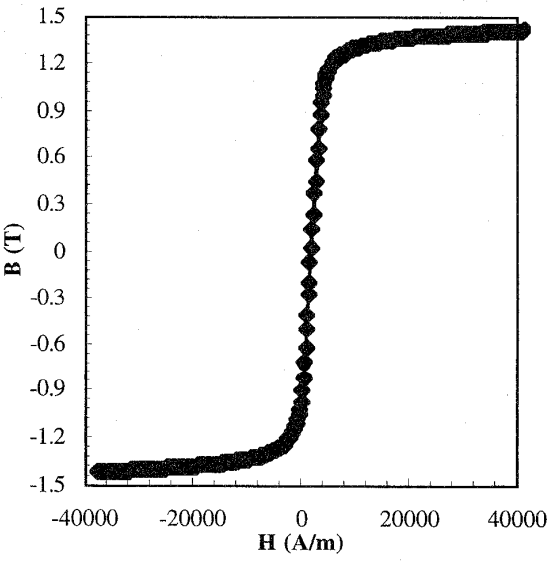

Figure 3. Flux density versus magnetic field intensity curve for fabricated orthonol (50/50) test samples

As can be seen, both materials exhibit a relatively high permeability. The saturation flux density for these electroplated permalloy samples is approximately 0.95 Tesla, whereas the saturation flux density for these orthonol samples is approximately 1.4 Tesla. From equation 5, this 40% increase in saturation flux density for orthonol-based magnetic components translates directly to a 40% increase in saturation current. In order to assess this effect in actual application, inductive components based on both permalloy and orthonol were fabricated and tested.

FABRICATION

In order to achieve the inductive component shown in Figure 1, several issues must be examined. The metal interconnections which are used to construct the 'wrapping coils' include metal via contacts. These via contacts may produce a relatively high metal contact resistance which causes high coil resistance and low Q-factor. If more coil turns are required to achieve high inductance, more via contacts should be added. To address this problem, electroplating techniques are used to fabricate the conductor lines and the vias, as electroplated metal contacts usually have a relatively low metal contact resistance [13].

Among several obstacles encountered in fabricating this micromachined inductive component, the major difficulty comes from the fabrication of thick wrapping coils which have a low conductor resistance. Thick molds for the wrapping coils are patterned using thick photoresist and photolithography. Electroplating is a favorable technique for deposition of the thick metal conductor, but electroplating usually requires a plating seed layer which must be removed after completing the fabrication structure. Consequently, the seed layer used for the lower conductor lines should serve as the plating seed layer for the via and remain until the micromachined inductor fabrication is completed. The seed layer must be removed after serving as a seed layer for electroplating, or all of the coils will be shorted. Unfortunately, the seed layer is now difficult to remove, as it is at the bottom of the structure. Simple blanket etching to expose the seed layer will not work as the magnetic core placed on the top of the lower conductors serves as a mask to prevent complete exposure of the seed layer. To solve this problem, a mesh-type seed layer [12] as depicted in Figure 4 can be used. This mesh-type seed layer can serve as the electroplating seed layer for the lower conductor lines and vias until the fabrication is completed. When the fabrication of this device is finished, the edges of the mesh seed layer can be exposed using plasma etch and then removed, ensuring the electrical isolation of the coils.

Another difficulty in the fabrication comes from the need to fabricate a thick magnetic core (for low magnetic reluctance) which should be placed on the top of the insulated lower conductor lines. The relatively high aspect ratio of the magnetic core causes a serious difficulty in patterning the conductor vias and the upper conductor lines, due to poor planarization of the surface. Optimal fabrication sequence design is required to solve these problems.

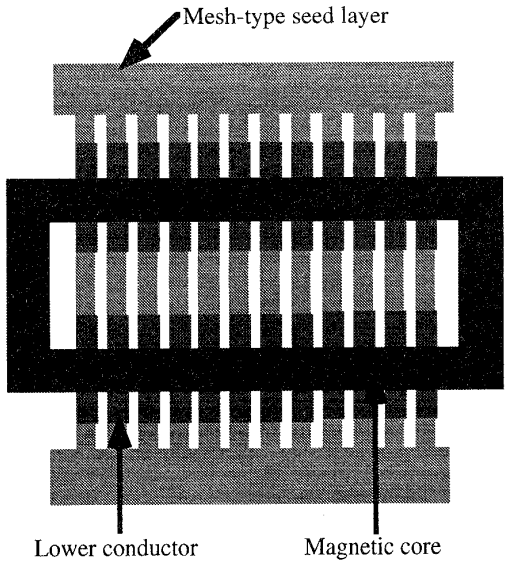

Figure 4. Mesh-type seed layer to serve as a plating seed layer and to be removed after the completion of fabrication

A brief fabrication process of this component is shown in Figure 5. The process started with an oxidized (0.4 μm thick SiO_2) 2-inch <100> silicon wafer as a substrate. Onto this substrate, chromium / copper / chromium layers were deposited to form an seed layer for electroplating using electron-beam evaporation. This mesh-type seed layer was patterned to form a conductor network to be removed after serving as the seed layer for plating of the conductor and vias. Polyimide (Dupont PI-2611) was spun on the top of mesh-type seed layer to construct electroplating molds for the bottom conductor lines. Four coats were made to obtain 40 μm thick polyimide molds. After coating of the polyimide, the polyimide was cured at 350 °C for 1 hour in nitrogen. An aluminum layer (0.3 μm thick) was deposited on top of the cured polyimide as a hard mask for dry etching. Molds for lower conductor lines (40 μm thick) were patterned on top of the deposited aluminum and etched using an O_2 (100%) plasma etch until the chromium / copper/ chromium seed layer was exposed. After etching the aluminum hard mask and the top chromium of the seed layer, the electroplating molds were filled with electroplated copper using standard copper electroplating techniques and the copper electroplating solution shown in Table I.

One coat of polyimide was cast to isolate bottom conductor lines and magnetic core. The seed layer, chromium / copper / chromium, for plating the magnetic core was deposited and coated with thick photoresist (Shipley STR 1110). Thick molds for the magnetic core were patterned and filled with plated nickel-iron after removing the top seed layer. The nickel-iron alloy plating solutions and conditions are shown in Table I. To plate the orthonol core (Ni (50%)-Fe (50 %) alloy), various additives from M&T Chemicals, Inc. were optionally used to control internal stress and ductility of the deposit, to keep the iron content solublized, and to obtain bright film and leveling of the

process. The pH and temperature should be kept within the recommended limits. A higher value may cause highly stressed deposits and a lower value may reduce leveling and cause chemical dissolving of iron anodes resulting in disruption of the bath equilibrium. Higher than recommended temperatures may give hazy deposits; much lower temperature may cause high current density burning. Air agitation and saccharin were also added to reduce internal stress and to keep the iron content stabilized. Upon completion of the electroplating, the seed layer was removed using wet etching.

Table I. Composition of nickel-iron and copper electroplating solutions

Nickel-iron electroplating solutions		
Component	Fe (20%)	Fe (50%)
$NiSO_4$-$6H_2O$	200 (g/l)	168 (g/l)
$FeSO_4$-$7H_2O$	8 (g/l)	81 (g/l)
$NiCl_2$-$6H_2O$	5 (g/l)	135 (g/l)
H_3BO_3	25 (g/l)	50 (g/l)
Saccharin	3 (g/l)	3 (g/l)
PH	2.5 ~ 3.0	3.5 ~ 4.0
Temperature	25 ~ 30 (°C)	55 ~ 60 (°C)
Copper electroplating solution		
Component	Quantity	
$CuSO_4$-$5H_2O$	250 (g/l)	
H_2SO_4	25 (ml/l)	

To insulate the core, additional polyimide was deposited in multiple coats and cured. Via holes were then dry etched through the polyimide layer using 100% oxygen plasma and an aluminum hard mask. Upon completion of the via etching, the aluminum hard mask was removed. To remove the oxidation caused during the etching of via holes, the exposed area of the lower conductor lines was etched in sulfuric acid (2%) solution for a few seconds. Vias were filled with plated copper, and then chromium / copper / chromium layer was deposited again. Molds for the top conductor lines were formed using thick photoresist STR 1110. The upper conductor lines were plated through the defined molds using the same plating conditions described above. After removing the photoresist, the plating seed layer for the top conductor lines was wet etched. After etching the seed layer, a polyimide passivation layer was deposited to protect the top conductor lines. The polyimide was optionally masked and etched to the bottom. The bottom mesh seed layer was then wet etched. At the completion of fabrication, samples were diced and tested. Figure 6 shows a micromachined inductor which consists of electroplated copper conductor lines (40 μm thick), an electroplated magnetic core (15 μm thick), and polyimide PI-2611 as an insulation material. Figures 7 and 8 show wrapped conductors and magnetic core through scanning electron micrographs taken after removing the polyimide using dry-etching. The interconnection of top conductors, vias, and lower conductors of the micromachined inductor is shown in Figure 9.

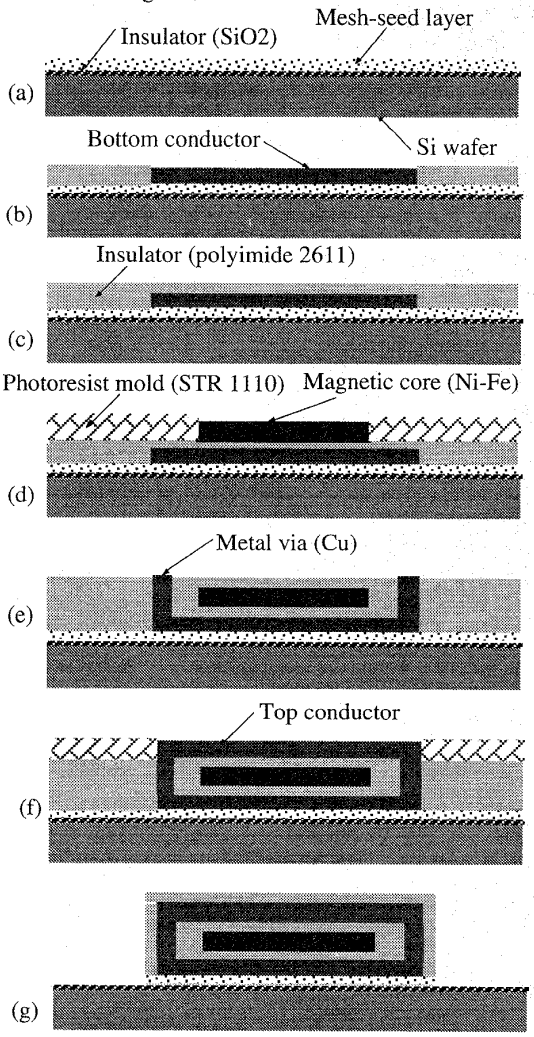

Figure 5. Fabrication steps of micromachined inductor: (a) patterning of mesh seed layer; (b) electroplating of bottom conductors; (c) Coating of polyimide; (d) magnetic core plating; (e) via conductor plating; (f) upper conductor plating; (g) removal of polyimide and mesh seed layer

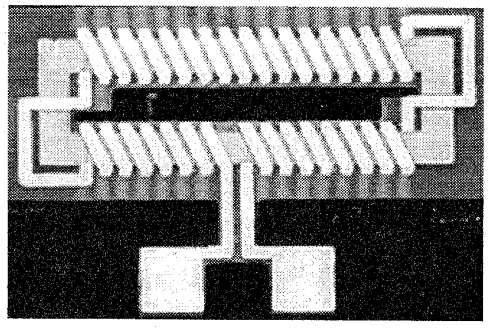

Figure 6. Photomicrograph of micromachined inductor

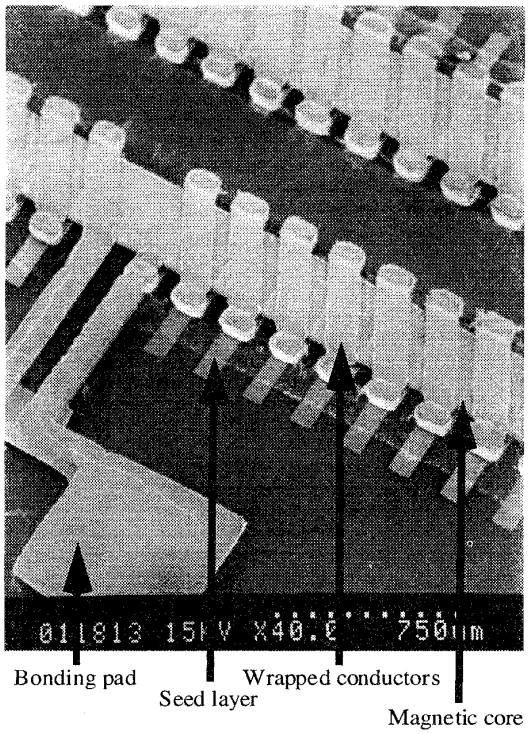

Figure 7. Scanning electron micrograph of the top view of micromachined inductor

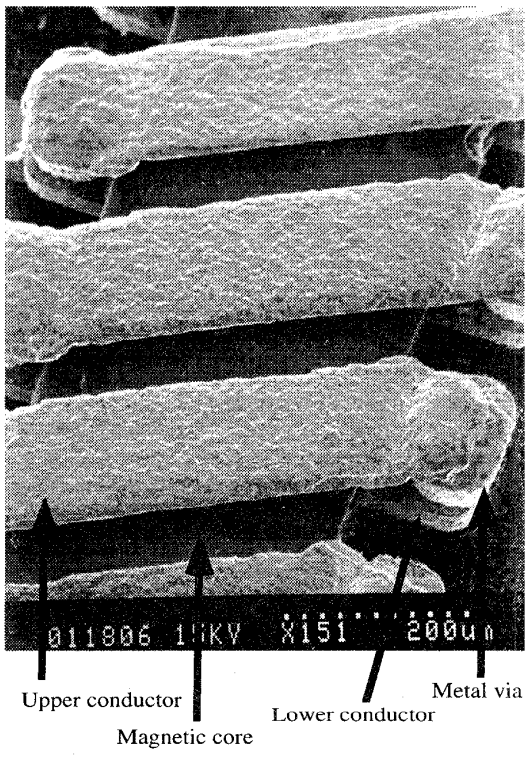

Figure 8. Scanning electron micrograph of wrapped conductors and a magnetic core of micromachined inductor

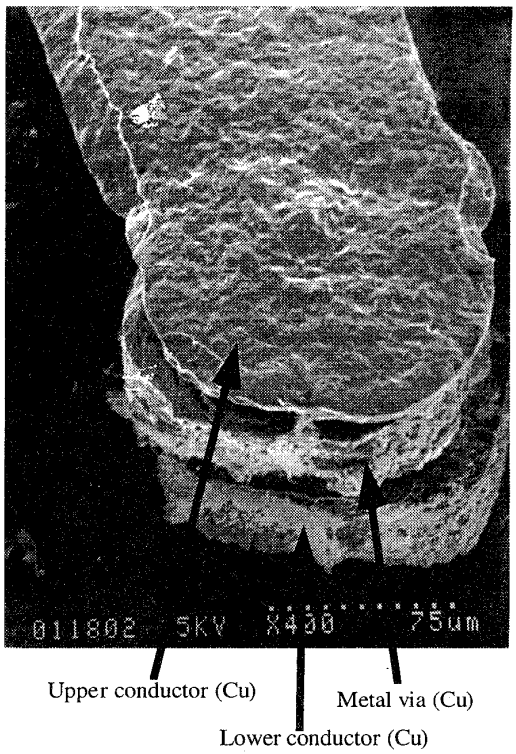

Figure 9. Scanning electron micrograph side view of the micromachined inductor

EXPERIMENTAL RESULTS AND ANALYSIS

For an inductor size of 4mm x 1.0mm x 0.13mm thickness having 30 turns of multilevel coils, the achieved inductances were approximately 0.67 μH for the inductor with permalloy core and 0.57 μH for the inductor with orthonol core at low frequencies. Inductance as a function of both frequency and DC current were measured using a Wayne kerr 3245 precision inductance analyzer. Figure 10 shows the inductance and Q-factor of each device as a function of frequency. As seen, the permalloy core inductor has a slightly higher inductance and Q-factor than the orthonol core inductor. The measured DC resistance of both inductors was approximately 0.3 ohms. This is very consistent with the value (0.309 ohms) evaluated from its geometry (neglecting via resistance) and the bulk value of copper conductivity. Although the individual via contact resistance was not measured, the excellent agreement between measured and calculated total resistance indicates that the via resistance is negligibly small. Thus, the electroplated via as predicted has avoided the high via resistance problem.

To find the circuit parameters of the integrated inductors, an equivalent circuit is assumed in which a stray capacitance [14] is in parallel with the series connection of the inductance and the internal resistance as shown in Figure 11. The resistance and stray capacitance of the inductors are derived from the measured impedance and phase as a function of frequency using equivalent circuit analysis and data collected from a Hewlett-Packard

impedance / gain-phase analyzer 4194A. Figures 12 and 13 show the gain and the phase shift of the micromachined inductors with permalloy and orthonol cores, respectively. Over the frequency range of a few hundred Hz to 10 MHz, the micromachined inductors display behavior similar to that of conventional inductors, with impedance increasing linearly with frequency and phase shifts near 90°. From these data, it can be concluded that winding capacitance and other parasitic capacitances do not appear to significantly affect inductor performance over the frequency ranges measured. The effect of the inductance fall off at higher frequencies shown in Figure 10 is due almost entirely to the dependence of the permeability of the magnetic core material on frequency.

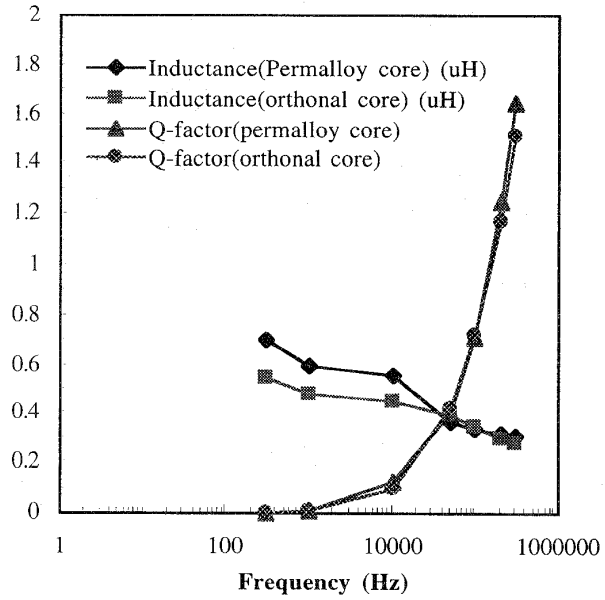

Figure 10. Comparison of the inductance and the Q-factor of micromachined inductors with different magnetic cores

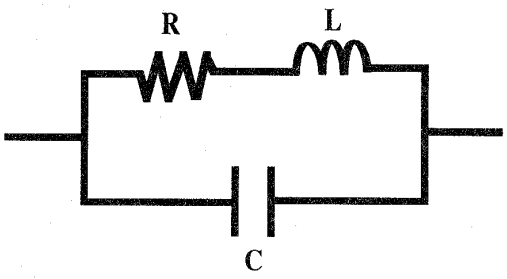

Figure 11. Equivalent circuit of the micromachined inductor used to analyze circuit parameters

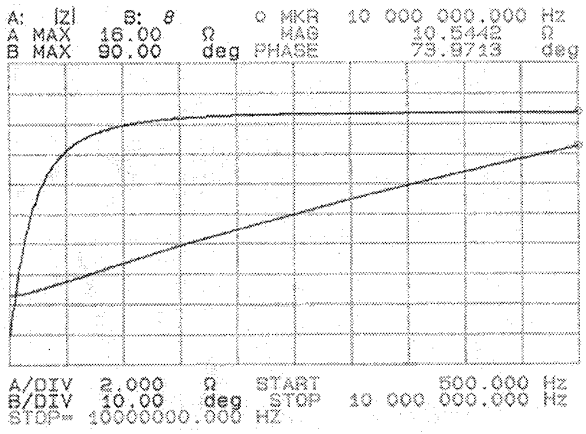

Figure 12. Impedance and phase analysis of micromachined inductor with permalloy core

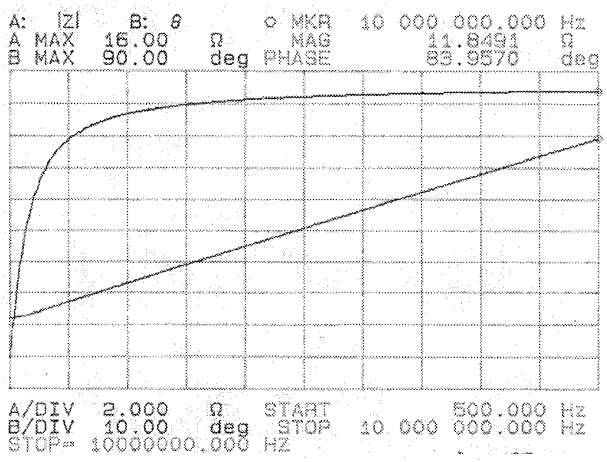

Figure 13. Impedance and phase analysis of micromachined inductor with orthonol core

Figure 14 shows the inductance of each inductor as a function of DC current. The inductance was measured when DC current was applied to each inductor. DC saturation current means the current at the point of inductance falloff. DC saturation current is generally defined as the current at which the inductance value falls off 20 ~ 30 % of the measured inductance without the applied DC current. The DC saturation current of the orthonol core inductor is much higher than the permalloy core inductor. From these data it can be concluded that orthonol-core inductors may perform significantly better than permalloy-core inductors in applications requiring magnetic energy storage, such as DC/DC converters.

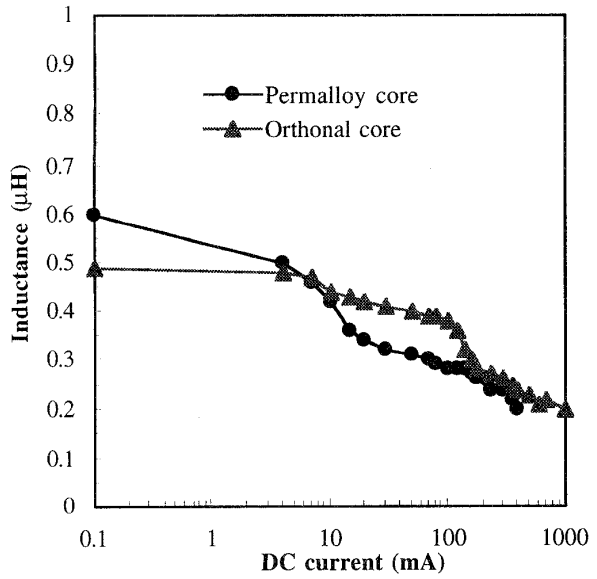

Figure 14. DC saturation current comparison of micromachined inductors with different magnetic cores

CONCLUSION

Fully integrated micromachined inductors with different magnetic cores have been realized on silicon wafers using micromachining and multilevel metallization techniques. In this paper, orthonol core inductors have been compared with permalloy core inductors to find a appropriate micromachined inductor for high power applications. As predicted, geometrically similar orthonol core inductors have much higher DC saturation current than permalloy core inductors, which is a very important characteristic for power inductors. These micromachined inductors have potential application as integrated passives for multichip modules, in which filters, DC/DC power converters, and micro-magnetic actuators and sensors integrated with the package are realized.

ACKNOWLEDGMENT

This research was supported by the National Science Foundation through the Georgia Tech / NSF Engineering Research Center in Electronic Packaging (contract EEC-9402723). Materials donations by E.I. DuPont de Nemours & Co. and M&T Chemicals Inc. are also gratefully acknowledged. Microfabrication was carried out at the Microelectronics Research Center of Georgia Tech with the assistance of the staff. Assistance with measurement of magnetic properties of materials from Mr. William Taylor of Georgia Tech as well as Mr. Michael Schneider and Professor Henry Baltes of the Swiss Federal Institute of Technology (ETH-Zürich) are gratefully acknowledged. Valuable technical discussions with Professor C. H. Ahn of the University of Cincinnati and the micromachining group at Georgia Tech are greatly appreciated.

REFERENCES

[1] C. H. Ahn, Y. J. Kim, and Mark G. Allen, "A fully integrated planar toroidal inductor with a micromachined Ni-Fe magnetic bar", *IEEE Transactions on Components, Hybrids and Manufacturing Technology*, 1993

[2] C. H. Ahn and M. G. Allen, " A fully integrated surface micromachined magnetic microactuator with a multilevel meander magnetic core", *IEEE J. Microelectromech. Syst.*, vol. 2, no. 1, pp. 15 ~ 22, 1993

[3] H. M. Greenhouse, "Design of planar rectangular microelectronic inductors", *IEEE Transactions Parts, Hybrids, and Packaging*, vol. PHP-10, no.2, pp.101 ~ 109, 1974

[4] O. Oshiro, H. Tsujimoto, and K. Shirae, "A novel miniature planar inductor", *IEEE Transactions on Magnetics*, vol. 23, no. 2, pp. 3759 ~ 3761, 1987

[5] R. F. Soohoo, "Magnetic thin film inductor for integrated circuit application", *IEEE Transactions on Magnetics*, vol. MAG-15, pp. 1803 ~ 1805, 1979

[6] K. Kawabe, H. Koyama, and K. Shirae, "Planar inductor", *IEEE Transactions on Magnetics*, vol. MAG-20, pp. 1804~ 1806, 1984

[7] M. Yamaguichi, M. Matsumoto, H. Ohzeki, and K. I. Arai, "Fabrication and basic characteristics of dry-etched micro inductors", *IEEE Transactions on Magnetics*, vol. MAG-26, pp. 2014 ~ 2016, 1990

[8] K. Mizuguchi and K. Yamasawa, "An on-board-type micro-switching converter with Mhz band-operation", *IEEE Translation Journal on Magnetics in Japan*, vol. 9, no. 2, pp. 174 ~ 178, 1994

[9] T. Sato, M. H. Tomita, A. Sawabe, T. Inoue, T. Mizoguchi, and M. Sahashi, "A magnetic thin film inductor and its application to a MHz switching dc-dc converter", *IEEE Transactions on Magnetics*, vol. 30, no. 2, pp. 217 ~ 223, March 1994

[10] T. Sato, M. Hasegawa, T.Mizoguchi, and M. Sahashi, "Study of high power planar inductor", *IEEE Transactions on Magnetics*, vol. 27, pp. 5277 ~ 5279, 1991

[11] H. Nishimura, I. Kamei, K. Shirakawa, Y. Kobayashi, O. Nakajima, and K. Murakami, "Studies on frequency characteristics of micro inductors", *IEEE Transactions on Magnetics*, vol. 9, no. 3, pp. 76 ~ 82, May 1994

[12] Colonel Wm. T. Mclyman, "Transformer and inductor design handbook", Second edition, pp. 20 ~ 25, 1988

[13] C. H. Ahn, "Micromachined components as integrated inductors and magnetic microactuators", *Ph. D. Thesis*, Georgia Institute of Technology, pp. 66 ~ 80, May, 1993

[14] M. Yamaguchi, M. Matsumoto, H. Ohzeki, and K. I. Arai, "Analysis of the inductance and the stray capacitance of the dry-etched micro inductors", *IEEE Transactions on Magnetics*, vol. 27, no. 6, pp. 5274 ~ 5276, 1991